

Edinburgh 97-15
 FTUV/98-1
 IFIC/98-1
 Rome Preprint 1182/97
 SNS/PH/1998-001

Lattice quark masses: a non-perturbative measurement.

V. Giménez

*Dep. de Física Teòrica and IFIC, Univ. de València,
 Dr. Moliner 50, E-46100, Burjassot, València, Spain*

L. Giusti

*Scuola Normale Superiore, P.zza dei Cavalieri 7 - I-56100 Pisa Italy
 INFN Sezione di Pisa I-56100 Pisa Italy*

F. Rapuano

*Dipartimento di Fisica, Università di Roma 'La Sapienza' and
 INFN, Sezione di Roma, P.le A. Moro 2, I-00185 Roma, Italy.*

M. Talevi

*Department of Physics and Astronomy, University of Edinburgh
 The King's Buildings, Edinburgh EH9 3JZ, UK.*

Abstract

We discuss the renormalization of different definitions of quark masses in the Wilson and the tree-level improved SW-Clover fermionic action. Using perturbative and non-perturbative renormalization constants, we study quark masses in the \overline{MS} scheme from Lattice QCD in the quenched approximation at $\beta = 6.0$, $\beta = 6.2$ and $\beta = 6.4$ for both actions. A reliable extrapolation to the continuum limit is however not yet possible. The most reliable results are: $\overline{m}^{\overline{MS}}(2\text{ GeV}) = 5.7 \pm 0.1 \pm 0.8\text{ MeV}$, $m_s^{\overline{MS}}(2\text{ GeV}) = 130 \pm 2 \pm 18\text{ MeV}$ and $m_c^{\overline{MS}}(2\text{ GeV}) = 1662 \pm 30 \pm 230\text{ MeV}$.

PACS: 11.15.H, 12.38.Gc, 13.30.Eg, 14.20.-c and 14.40.-n

1 Introduction

Quark masses are among the least known fundamental parameters of the Standard Model. Due to confinement, they cannot be measured directly and our knowledge of these quantities relies on techniques like Chiral perturbation theory (ChPT) [1], QCD Sum Rules (QCDSR) [2]-[5] and Lattice QCD (LQCD) [6]-[12]. ChPT gives rather precise determinations of ratios of quark masses while QCDSR and LQCD determine their absolute values. Moreover LQCD does not require model parameters or ad-hoc assumptions. Each technique suffers from different sources of errors that should be carefully studied. In the most recent LQCD simulations the main errors are due to the quenched approximation (i), the reach of the continuum limit (ii) and a correct matching of the lattice quantities to the continuum ones (iii). In this paper we try to overcome as much as possible the last problem. We define quark masses through the Vector and Axial Vector Ward Identities and discuss the renormalization procedure. We compute light, strange and charm quark masses with perturbative (PT) and non-perturbative (NP) renormalization constants (RC) using the Wilson and the tree-level improved Sheikholeslami-Wohlert (SW) Clover action [13], [14] which, in the following, we will be referring to as Improved Action. We also try to estimate the remaining overall systematic uncertainty, mainly due to (i) and (ii), comparing the chiral behaviour of the pseudoscalar and vector meson masses with the experimental ones.

The main result of this paper is a new measurement of the quark masses which we believe to be more reliable than previous ones.

The paper is organized as follows. In section 2 we discuss the theoretical definitions of lattice quark masses and the renormalization procedures. In section 3 we relate lattice quantities to the continuum ones and we review the NP renormalization of bilinear operators. In section 4 we give the details of the lattices used to extract masses and matrix elements. In section 5 we report our results on quark masses in the \overline{MS} -scheme and finally we give our conclusions.

2 Quark Masses

The usual on-shell mass definition cannot be used for quarks since they do not appear as physical states. Thus the values of the quark masses depend on the definition adopted. In the following we will give results for quark masses in the \overline{MS} scheme.

The quark mass can be defined by the perturbative expansion of the quark

propagator renormalized at a scale μ . This is equivalent to the definition from the renormalized Vector and Axial Ward Identities, which can be used to give a fully non-perturbative determination of the quark mass.

2.1 Quark masses from the Vector Ward Identity

Quark masses can be defined from the Vector Ward Identity (VWI). We first consider the Wilson formulation and then describe the Clover Improved case. The Vector Ward Identity between on-shell hadronic states α and β , neglecting terms of $O(a)$, can be written as [15]

$$\langle \alpha | \partial^\mu \tilde{V}_\mu^a | \beta \rangle = \langle \alpha | \bar{\psi} \left[\frac{\lambda^a}{2}, M \right] \psi | \beta \rangle \quad (1)$$

where ψ is a flavour triplet of bare quark fields q_i , M is the quark bare mass matrix, $\lambda^a/2$ are the generators of the $SU(3)$ flavour group normalized by $Tr[\lambda^a \lambda^b] = 2 \delta^{ab}$ and the derivative ∂^μ is the usual asymmetric lattice derivative. The conserved vector current \tilde{V}_μ^a is:

$$\begin{aligned} \tilde{V}_\mu^a(x) = \frac{1}{2} \left[\bar{\psi}(x) (\gamma_\mu - 1) U_\mu(x) \frac{\lambda^a}{2} \psi(x + \mu) \right. \\ \left. + \bar{\psi}(x + \mu) (\gamma_\mu + 1) U_\mu^\dagger(x) \frac{\lambda^a}{2} \psi(x) \right] \end{aligned} \quad (2)$$

and its renormalization constant satisfies $Z_{\tilde{V}} = 1$. U_μ are the link variables on the lattice. By taking the linear combination $\tilde{V}_\mu = \tilde{V}_\mu^1 - i\tilde{V}_\mu^2$ we obtain:

$$\langle \alpha | \partial^\mu \tilde{V}_\mu | \beta \rangle = \frac{1}{2} \left(\frac{1}{k_2} - \frac{1}{k_1} \right) \langle \alpha | S | \beta \rangle \quad (3)$$

where k_i is the hopping parameter of i -th quark, $S = \bar{q}_2 q_1$ is the bare scalar density.

On the lattice the ratio of the vector and scalar matrix elements could be used to determine quark masses. Unfortunately the scalar matrix element turns out to be extremely noisy, preventing any reliable analysis. We then use eq.(3) only to fix the relation between the lattice bare quark mass in lattice units and the hopping parameter, i.e.

$$m_i = \frac{1}{2} \left(\frac{1}{k_i} - \frac{1}{k_c} \right) \quad (4)$$

where k_c is the critical value of the hopping parameter. Eq. (3) shows that the quark mass, defined in (4), is renormalized with $Z_S^{-1} = Z_m$, where Z_S is the renormalization constant of the scalar density. For the pseudoscalar and vector meson masses as a function of quark masses, ChPT gives

$$M_{PS}^2 = C(m_1 + m_2) , \quad (5)$$

$$M_V = A + B(m_1 + m_2) . \quad (6)$$

From equations (5) and (6) one can extract the bare lattice quark mass of a given flavour. This is the so called ‘‘spectroscopy method’’.

In the Improved case eq. (3) will be more complicate as other terms will appear due to our use of ‘‘ \not{D} -rotated operators’’ [14]:

$$q_i \longrightarrow \left\{ 1 - \frac{1}{2} [z \not{D} - (1 - z) m_i] \right\} q_i \quad (7)$$

where \not{D} is the lattice covariant derivative, i denotes the flavour of the quark field and z is an arbitrary real number. For $z = 0$, each field q_i is multiplied by a numerical factor so that the tree-level improved bilinear operators are simply [16]

$$O_\Gamma^I = (1 + m_i) O_\Gamma , \quad (8)$$

obtaining, as for eq. (3),

$$\begin{aligned} \langle \alpha | \bar{\partial}^\mu \tilde{V}_\mu^I | \beta \rangle = & \quad (9) \\ \frac{1}{4} (m_2^I - m_1^I) \langle \alpha | (2S^I(x) + S^I(x + \hat{0}) + S^I(x - \hat{0})) | \beta \rangle , & \end{aligned}$$

with the symmetric derivative $\bar{\partial}_\mu f(x) = (f(x + \mu) - f(x - \mu))/2a$ [17], where a is the lattice spacing.

However, one should note that the combination of scalar densities in the right hand side of eq. (9) can be replaced by $S^I(x)$ up to higher orders in the lattice spacing a . From eqs. (8)-(9) and the fact that the Clover Improved action has only $O(ag^2)$ errors, we obtain that the mass m_i^I , improved up to $O(ag^2)$, is

$$m_i^I = \frac{1}{2} \left(\frac{1}{k_i} - \frac{1}{k_c} \right) \left[1 - \frac{1}{4} \left(\frac{1}{k_i} - \frac{1}{k_c} \right) \right] . \quad (10)$$

Eq. (10) is, of course, the tree level approximation of the relation obtained in [18]. This procedure can be straightforwardly applied to the perturbative case

using RC's that do not contain the field “rotation” contribution, but not in the non perturbative one as, for historical reasons, we have computed RC's using “rotated” fields with $z = 1$.

2.2 Quark masses from the Axial Ward Identity

In this section we will describe the definition of the mass from the Axial Ward Identity (AWI). As for the VWI case we first consider the Wilson formulation and then describe the Clover Improved case. Close to the chiral limit and neglecting terms of $O(a)$, the Axial Ward Identity is [15]:

$$Z_A \langle \alpha | \partial^\mu A_\mu^a | \beta \rangle = \langle \alpha | \bar{\psi} \left\{ \frac{\lambda^a}{2}, M - \overline{M} \right\} \gamma_5 \psi | \beta \rangle, \quad (11)$$

where Z_A is the RC of the axial current and \overline{M} , defined in [15], in the chiral limit is the critical value of the quark mass. Following the same steps as for the VWI, and for the same flavour choice as in eq. (3), we obtain that one can extract quark masses from the ratio of matrix elements

$$\frac{1}{2}(\rho_1 + \rho_2) = \frac{\langle 0 | \partial_0 A_0 | PS(\vec{p} = 0) \rangle}{\langle 0 | P | PS(\vec{p} = 0) \rangle}, \quad (12)$$

where $A_\mu = \bar{q}_2 \gamma_\mu \gamma_5 q_1$, $P = \bar{q}_2 \gamma_5 q_1$ and PS is a pseudoscalar meson. This ratio is renormalized with Z_A/Z_P , where Z_P is the RC of the pseudoscalar density.

For the Clover improved case, the only difference is that we need to consider the ratio of improved operators and to take the symmetric derivative, as in eq. (9).

3 Renormalization of quark masses

In the continuum, “physical” quantities like for example quark masses and decay constants are defined specifying the renormalization prescription used to eliminate the divergences in the matrix elements of the operators determining them. The standard practice consists in choosing a Dimensional Regularization scheme, for instance, $NDR - \overline{MS}$. On the lattice, however, the matrix elements of the corresponding operators are regularized by introducing a hard cut-off, a^{-1} , in the momentum integrals. Since the continuum and lattice renormalization schemes, in general, differ, so do the corresponding amplitudes. Therefore, in order to convert the bare lattice values of amplitudes to

their continuum counterparts, we have to know the matching coefficient, the so-called lattice renormalization constant.

One method, which is described in section 3.1, consists in computing two amplitudes to a given order in perturbation theory in the continuum and on the lattice. Imposing that they must be equal after renormalization at a given scale, one finds the lattice RC's to some order in perturbation theory.

However, to avoid the use of perturbation theory on the lattice, a general method for the non-perturbative calculation of lattice RC's in the RI (regularization independent) scheme has been devised. We shall briefly discuss this in section 3.2. Once we have obtained the lattice RC's in the RI scheme non-perturbatively, the conversion to other continuum schemes like $NDR - \overline{MS}$ and the running of the continuum quantity to other scales can be calculated in perturbation theory at a given order.

3.1 The perturbative approach

In the perturbative approach one uses lattice and continuum perturbation theory at the next-to-leading order (NLO).

For the VWI definition, we have

$$\begin{aligned} m^{\overline{MS}}(\mu) &= U_m^{\overline{MS}}(\mu, \pi/a) \frac{1}{Z_S^{\overline{MS}}} m a^{-1} \\ &= U_m^{\overline{MS}}(\mu, \pi/a) \left[1 + \frac{\alpha_s(\pi/a)}{4\pi} K_{VWI} \right] m a^{-1} \end{aligned} \quad (13)$$

where m is the bare quark mass of a generic flavour,

$$K_{VWI} = -C_F(\Delta_S + \Delta_\Sigma) - \gamma^{(0)} \log(\pi), \quad (14)$$

$C_F = (N^2 - 1)/2N$ and N being the number of colours. Δ_S and Δ_Σ have been computed in ref. [16,19] and following them can be extracted from table 1 for both actions.

$$U_m^{\overline{MS}}(\mu, \pi/a) = \left(\frac{\alpha_s(\mu)}{\alpha_s(\pi/a)} \right)^{\gamma^{(0)}/2\beta_0} \left[1 + \frac{\alpha_s(\mu) - \alpha_s(\pi/a)}{4\pi} \left(\frac{\gamma^{(1)}}{2\beta_0} - \frac{\gamma^{(0)}\beta_1}{2\beta_0^2} \right) \right] \quad (15)$$

where the coupling constant is defined in the \overline{MS} scheme,

$$\begin{aligned}\beta_0 &= \frac{11N - 2n_f}{3} \\ \beta_1 &= \frac{34}{3}N^2 - \frac{10}{3}Nn_f - \frac{N^2 - 1}{N}n_f \\ \gamma^{(0)} &= 6\frac{N^2 - 1}{2N}\end{aligned}\tag{16}$$

$$\gamma^{(1)} = \frac{97N}{3}\frac{N^2 - 1}{2N} + 3\left(\frac{N^2 - 1}{2N}\right)^2 - \frac{10n_f}{3}\frac{N^2 - 1}{2N}\tag{17}$$

and n_f is the flavour number. In the improved case, as discussed before, Δ_S in eq. (14) should not include the contribution due to the rotation of the fields.

Analogously, for the AWI method, we have

$$\begin{aligned}m^{\overline{MS}}(\mu) &= U_m^{\overline{MS}}(\mu, \pi/a) \frac{Z_A^{\overline{MS}}}{Z_P^{\overline{MS}}} \rho a^{-1} \\ &= U_m^{\overline{MS}}(\mu, \pi/a) \left[1 + \frac{\alpha_s(\pi/a)}{4\pi} K_{AWI} \right] \rho a^{-1},\end{aligned}\tag{18}$$

where $\frac{\rho}{2}$ is the ratio defined in (12) for a generic flavour and

$$K_{AWI} = C_F(\Delta_A - \Delta_P) - \gamma^{(0)} \log(\pi).\tag{19}$$

Also Δ_A and Δ_P can be computed from table 1 following [16,19].

3.2 The non-perturbative approach

At scales $a^{-1} \simeq 2-4$ GeV, where a is the lattice spacing, of our simulations, we expect small NP effects on the renormalization constants of bilinear operators. However “tadpole” diagrams [20], which are present in lattice perturbation theory, can give rise to large corrections and then to large uncertainties in the matching procedure at values of $\beta = 6/g_L^2 = 6.0 - 6.4$. These problems are avoided using NP renormalization techniques [21,22]. Although the nature of the systematics changes in adopting a NP approach, mainly because of $O(a)$ effects as we shall discuss in [23], we believe that the NP determination of RC’s is more reliable.

We shortly review the NP method for the RC’s which enter the determination of the quark masses. For the full discussion of the method, the results obtained and their systematics we refer to a forthcoming paper [23].

Let us consider a quark bilinear $O_\Gamma = \bar{q}\Gamma q$, where Γ is a Dirac matrix and q now represents the generic lattice flavour-degenerate quark field. In this work we will consider the scalar and pseudoscalar densities and the Axial Vector current.

The renormalization conditions are imposed on the amputated Green functions computed between off-shell quark states of momentum p in the Landau gauge

$$\Lambda_O(pa) = S_q(pa)^{-1}G_O(pa)S_q(pa)^{-1} \quad (20)$$

where $G_O(pa)$ and $S_q(pa)$ are the non-amputated Green functions and the quark propagator, calculated non-perturbatively via Monte Carlo simulations [21]. Possible effects from Gribov copies or spurious solutions [24] have not been considered. The RC $Z_O^{RI}(\mu a, g_0)$ of O_Γ is determined by the condition

$$Z_O^{RI}(\mu a)Z_q^{-1}(\mu a)\text{Tr } \mathbf{P}_O\Lambda_O(pa)|_{p^2=\mu^2} = 1, \quad (21)$$

where \mathbf{P}_O is a suitable projector on the tree-level amputated Green function (normalized to 1) [21] and Z_q is the wave function RC which can be defined in different ways [21]. From the Ward Identities

$$Z_q(\mu a) = -i\frac{1}{12}\text{Tr}\left(\frac{\partial S_q(pa)^{-1}}{\partial \not{p}}\right)\Bigg|_{p^2=\mu^2}. \quad (22)$$

To avoid derivatives with respect to a discrete variable, we have used

$$Z'_q(\mu a) = -i\frac{1}{12}\frac{\text{Tr} \sum_{\mu=1,4} \gamma_\mu \sin(p_\mu a) S_q(pa)^{-1}}{4 \sum_{\mu=1,4} \sin^2(p_\mu a)}\Bigg|_{p^2=\mu^2}, \quad (23)$$

which, in the Landau Gauge, differs from Z_q by a finite term of order α_s^2 which is irrelevant at the NLO.

For this procedure to be reliable μ must satisfy the condition $\mu \ll 1/a$ to avoid discretization errors but also $\mu \gg \Lambda_{QCD}$ to avoid non-perturbative effects or higher order corrections in the continuum perturbative expansion.

The quark mass in the \overline{MS} scheme is then defined as

$$m^{\overline{MS}}(\mu) = U_m^{\overline{MS}}(\mu, \mu') \left[1 + \frac{\alpha_s(\mu')}{4\pi} C_m^{LAN} \right] m^{RI}(\mu'), \quad (24)$$

| Regularization | Δ_Σ | Δ_S^{Loc} | Δ_S^\otimes | Δ_P^{Loc} | Δ_P^\otimes | Δ_A^{Loc} | Δ_A^\otimes |
|----------------|-----------------|------------------|--------------------|------------------|--------------------|------------------|--------------------|
| Wilson | -12.85 | -0.10 | - | -9.78 | - | -3.0 | - |
| Clover | -9.2 | -10.07 | 12.0 | -13.1 | -4.3 | -4.6 | 11.7 |

Table 1
Coefficients entering the perturbative matching of the quark masses.
where [21]

$$C_m^{LAN} = -4 \frac{N^2 - 1}{2N} \quad (25)$$

and for $m^{RI}(\mu')$ we get

$$m^{RI}(\mu') = \frac{1}{Z_S^{RI}(\mu'a)} m a^{-1}$$

$$m^{RI}(\mu') = \frac{Z_A^{RI}}{Z_P^{RI}(\mu'a)} \frac{\rho}{2} a^{-1} \quad (26)$$

for the Vector and Axial Vector WI respectively. As both the RI and the \overline{MS} respect chirality we have $Z_A^{RI} = Z_A$.

This discussion applies immediately to the unquenched case [25].

4 Details of the analysis

In this section we describe the extraction of meson masses, matrix elements and lattice quark masses from the two point correlation functions and the interpolation/extrapolation of the results in the heavy and light quark masses to the physical points. We also try to estimate the overall systematic errors on the lattice quark masses.

4.1 Lattice details

In this work we have used various lattices that have been generated by the APE group in the last years. Tables 2 and 3 show the parameters of the lattices that we have analyzed. A more detailed discussion of lattice calibration and spectroscopy can be found in [7] for the light quark systems and in [26] for the heavy-light ones. Here we will just summarize the most important points.

Meson masses and axial-pseudoscalar matrix elements have been extracted from two-point correlation functions in the standard way from the following propagators

$$\begin{aligned} G_{55}(t) &= \sum_x \langle P(x, t) P^\dagger(0, 0) \rangle , \\ G_{05}(t) &= \sum_x \langle A_0(x, t) P^\dagger(0, 0) \rangle \end{aligned} \quad (27)$$

and

$$G_{ii}(t) = \sum_{i=1,3} \sum_x \langle V_i(x, t) V_i^\dagger(0, 0) \rangle , \quad (28)$$

where

$$\begin{aligned} P(x, t) &= \bar{q}(x, t) \gamma_5 q(x, t) , \\ A_\mu(x, t) &= \bar{q}(x, t) \gamma_\mu \gamma_5 q(x, t) , \\ V_i(x, t) &= \bar{q}(x, t) \gamma_i q(x, t) . \end{aligned}$$

where q represents the generic lattice flavour-degenerate quark field and i is a spatial index. We fit the zero-momentum correlation functions in eqs. (27) and (28) to a single particle propagator

$$\begin{aligned} G_{55}(t) &= \frac{Z^{55}}{M_{PS}} \exp\left(-\frac{1}{2} M_{PS} T\right) \cosh\left[M_{PS} \left(\frac{T}{2} - t\right)\right] , \\ G_{ii}(t) &= \frac{Z^{ii}}{M_V} \exp\left(-\frac{1}{2} M_V T\right) \cosh\left[M_V \left(\frac{T}{2} - t\right)\right] , \end{aligned} \quad (29)$$

in the time intervals reported in tables 2 and 3. In (29), T represents the lattice time extension, the subscripts PS and V stand for pseudoscalar and vector mesons. To improve stability, the meson (axial-pseudoscalar) correlation functions have been symmetrized (anti-symmetrized) around $t = T/2$. The time intervals for the fits are chosen with the following criteria: we fix the lower limit of the interval as the one at which there is a stabilization of the effective mass, and, as the upper limit, the furthest possible point before the error overwhelms the signal. The errors have been estimated by a jack-knife procedure, blocking the data in groups of 10 configurations and we have checked that there are no relevant changes in the error estimate by blocking groups of configurations of different size.

| | C60a | C60b | C60c | C60d | C62a | C64 |
|---------------|--------------------|------------------|------------------|------------------|------------------|------------------|
| β | 6.0 | 6.0 | 6.0 | 6.0 | 6.2 | 6.4 |
| # Confs | 490 | 600 | 200 | 200 | 250 | 400 |
| Volume | $18^3 \times 64$ | $24^3 \times 40$ | $18^3 \times 32$ | $16^3 \times 32$ | $24^3 \times 64$ | $24^3 \times 64$ |
| k_l | 0.1425 | 0.1425 | 0.1425 | 0.1425 | 0.14144 | 0.1400 |
| | 0.1432 | 0.1432 | 0.1432 | 0.1432 | 0.14184 | 0.1403 |
| | 0.1440 | 0.1440 | 0.1440 | 0.1440 | 0.14224 | 0.1406 |
| | - | - | - | - | 0.14264 | 0.1409 |
| k_h | - | - | - | - | 0.1210 | - |
| | - | - | - | - | 0.1250 | - |
| | - | - | - | - | 0.1290 | - |
| | - | - | - | - | 0.1330 | - |
| | Light-light mesons | | | | | |
| $t_1 - t_2$ | 15-28 | 15-19 | 11-15 | 11-15 | 18-28 | 24-30 |
| | Heavy-light mesons | | | | | |
| $t_1 - t_2$ | - | - | - | - | 20-28 | - |
| $a^{-1}(K^*)$ | 2.12(6) | 2.16(4) | 2.07(6) | 2.23(9) | 2.7(1) | 4.0(2) |

Table 2

Summary of the parameters of the runs with the SW-Clover fermion action analyzed in this work.

We extract ρ from the ratio

$$\rho = \frac{\langle \partial_0 A_0(t) P(0) \rangle}{\langle P(t) P(0) \rangle} \quad (30)$$

at zero spatial momentum. At large time separations, we fit the ratio $G_{05}(t)/G_{55}(t)$ and we get

$$\rho = \sinh(M_{PS}) \frac{\langle A_0(t) P(0) \rangle}{\langle P(t) P(0) \rangle} \quad (31)$$

in a t region where the signal stabilizes. The hyperbolic sine comes from the discrete symmetric derivative which is necessary to consistently take into account $O(a)$ terms.

Tables 2 and 3 also contain the values of the lattice spacing a extracted from

| | W60 | W62a | W62b | W64 |
|---------------|--------------------|------------------|------------------|------------------|
| β | 6.0 | 6.2 | 6.2 | 6.4 |
| # Confs | 320 | 250 | 110 | 400 |
| Volume | $18^3 \times 64$ | $24^3 \times 64$ | $24^3 \times 64$ | $24^3 \times 64$ |
| k_l | 0.1530 | 0.1510 | 0.1510 | 0.1488 |
| | 0.1540 | 0.1515 | - | 0.1492 |
| | 0.1550 | 0.1520 | 0.1520 | 0.1496 |
| | - | 0.1526 | 0.1526 | 0.1500 |
| k_h | 0.1255 | 0.1300 | 0.1300 | - |
| | 0.1320 | 0.1350 | 0.1350 | - |
| | 0.1385 | 0.1400 | 0.1400 | - |
| | 0.1420 | 0.1450 | 0.1450 | - |
| | 0.1455 | - | 0.1500 | - |
| | Light-light mesons | | | |
| $t_1 - t_2$ | 15-28 | 18-28 | 18-28 | 24-30 |
| | Heavy-light mesons | | | |
| $t_1 - t_2$ | 15-28 | 20-28 | 20-28 | - |
| $a^{-1}(K^*)$ | 2.26(5) | 3.00(9) | 3.0(1) | 4.1(2) |

Table 3

Summary of the parameters of the runs with the Wilson action analyzed in this work.

the K^* mass with the "lattice physical plane" (lp-plane) method [7].

We have also performed dedicated runs at $\beta = 6.0, 6.2$ and 6.4 for both the Wilson and the SW-Clover actions to measure the RC's according to the discussion of section 3.2. The parameters of these runs and the results for Z_S^{RI} , Z_P^{RI} and Z_A^{RI} are reported in table 4.

4.2 Extraction of raw results for light and strange quarks

Once the hadronic correlation functions have been fitted, and the lattice masses and matrix elements extracted, we have to perform a number of interpolations/extrapolations to extract physical quantities.

We extract light and strange quark masses from the meson spectroscopy and from the Axial Ward Identity with three different methods:

| | | | | | | |
|-----------------------|------------------|------------------|------------------|------------------|------------------|------------------|
| β | 6.0 | 6.0 | 6.2 | 6.2 | 6.4 | 6.4 |
| Action | SW | Wilson | SW | Wilson | SW | Wilson |
| # Confs | 100 | 100 | 180 | 100 | 60 | 60 |
| Volume | $16^3 \times 32$ | $16^3 \times 32$ | $16^3 \times 32$ | $16^3 \times 32$ | $24^3 \times 32$ | $24^3 \times 32$ |
| k | 0.1425 | 0.1530 | 0.14144 | 0.1510 | 0.1400 | 0.1488 |
| | 0.1432 | 0.1540 | 0.14184 | 0.1515 | 0.1403 | 0.1492 |
| | 0.1440 | 0.1550 | 0.14224 | 0.1520 | 0.1406 | 0.1496 |
| | | | 0.14264 | 0.1526 | 0.1409 | 0.1500 |
| k_c | 0.14551 | 0.15683 | 0.14319 | 0.15337 | 0.14143 | 0.15058 |
| $Z_S^{RI}(m_q a = 0)$ | 0.834(18) | 0.682(9) | 0.851(11) | 0.722(8) | 0.852(13) | 0.742(8) |
| $Z_P^{RI}(m_q a = 0)$ | 0.409(8) | 0.447(5) | 0.466(4) | 0.499(5) | 0.555(6) | 0.572(4) |
| $Z_A^{RI}(m_q a = 0)$ | 1.047(18) | 0.808(7) | 1.023(4) | 0.812(6) | 1.012(9) | 0.825(6) |

Table 4

Parameters of the runs used in the non perturbative calculation of the renormalization constants and values of Z_S^{RI} , Z_P^{RI} and Z_A^{RI} at a scale $\mu a \simeq 1$. The errors reported are statistical only.

- (1) We define the physical plane [M_V , M_{PS}^2] (lp-plane [7]) and, assuming that only linear terms are important, we determine the lattice values M_K and M_{K^*} imposing that M_V/M_{PS} coincides with the experimental value $C_{sl} = M_{K^*}^{exp}/M_K^{exp}$ [27]. Comparing $M_{K^*} a^{-1}$ with its experimental value we extract the lattice spacing reported in tables 2 and 3. Using relations (5) and (4) and imposing the prediction of the CPTh [1]

$$R = \frac{m_s}{\bar{m}} = 24.4 \pm 1.5, \quad (32)$$

where $\bar{m} = (m_u + m_d)/2$, we obtain

$$m_s = \frac{M_K^2}{C(1 + 1/R)} \quad (33)$$

$$\bar{m} = \frac{m_s}{R}. \quad (34)$$

The lattice strange quark mass obtained with (33) for all lattices are reported in table 6.

In extracting the values of a^{-1} , M_K and C from our data, we assume that the relation between quark masses and squared pseudoscalar masses is linear up to the strange quark region (see eq.(2)), so we can compute these quantities using our data for quark masses in the ‘‘strange mass region’’ by interpolating only. In other words, no extrapolation to the light

quark region is performed. Possible deviations from linearity induced by terms of the form $D(m_s + \bar{m})^2 + D'(m_s - \bar{m})^2$ are known to be small and will give rise to uncertainties which can be neglected. Moreover, the value of k_c is not required to obtain the quark masses in the Wilson case. For the improved action, however, a small dependence of C on k_c exists because of the quadratic term in eq.(7). This gives rise anyway to quite small fluctuations.

For the Axial Ward Identity, in the same fashion, we define the plane $[\rho, M_{PS}^2]$, where ρ is defined in the equation (31), and we obtain

$$\rho_s = \frac{\rho|_{M_{PS}=M_K}}{(1 + 1/R)} \quad (35)$$

$$\bar{\rho} = \frac{\rho_s}{R} . \quad (36)$$

In this case, for both actions, there is no chiral extrapolation needed. The values of ρ_s for all lattices are reported in table 7.

- (2) On the physical plane $[M_V M_{PS}^2]$, we determine M_K and M_{K^*} as in (1) and M_π and M_ρ imposing that M_V/M_{PS} coincides with the experimental value $C_{ll} = M_\rho^{exp}/M_\pi^{exp}$. Using (5) and (4) we obtain

$$\bar{m} = \frac{M_\pi^2}{2C} \quad (37)$$

$$m_s = \frac{1}{C} \left(M_K^2 - \frac{M_\pi^2}{2} \right) . \quad (38)$$

The lattice light quark masses obtained with (37) for all lattices are reported in table 6. For the Axial Ward Identity we define the plane $[\rho, M_{PS}^2]$ and we obtain

$$\begin{aligned} \bar{\rho} &= \frac{1}{2}\rho \Big|_{M_{PS}=M_\pi} \\ \rho_s &= \rho|_{M_{PS}=M_K} - \frac{1}{2}\rho \Big|_{M_{PS}=M_\pi} . \end{aligned} \quad (39)$$

The values of $\bar{\rho}$ for all lattices are reported in table 7.

- (3) Using eqs. (4), (6) and the lattice spacing determined as in (1) we compare $(M_\phi a^{-1})$ to its experimental value and we obtain

$$m_s = \frac{M_\Phi^{exp} a - A}{2B} . \quad (40)$$

From (4) and (40) we determine k_s and then we use

$$\rho = G \left(\frac{1}{k} - \frac{1}{k_c} \right) \quad (41)$$

to determine ρ_s .

The three methods (1), (2) and (3) described above should give consistent values for \bar{m} , m_s , $\bar{\rho}$ and ρ_s , apart from discretization errors and quenching effects. It is well known [7,10] that the strange quark mass obtained from M_ϕ (3) is systematically higher than the value obtained from M_K (1).

The ratio of the strange quark masses obtained with different methods is connected to experimental quantities. From (5) and (6) we get

$$M_V = A + DM_{PS}^2 \quad (42)$$

where $D \cdot C = B$. A and D can be measured fitting linearly the experimental data on the meson masses [27]. To compare lattice data with experimental measurements we prefer to use two equivalent dimensionless quantities

$$J \equiv M_{K^*} \frac{dM_V}{dM_{PS}^2} = M_{K^*} D$$

$$L \equiv \frac{A}{M_{K^*}} . \quad (43)$$

In table 5 we report the experimental values and the lattice predictions we have obtained for J and L . One can see that J has quite large fluctuations and is also quite far from the experimental value. It has been argued [28] that this may be mainly due to the quenching approximation.

| Run | J | L | R_{m_s} |
|------|-----------|-----------|-----------|
| Exp. | 0.499 | 0.847 | 1 |
| C60a | 0.367(13) | 0.887(4) | 0.852(17) |
| C60b | 0.377(8) | 0.884(2) | 0.866(10) |
| C60c | 0.359(16) | 0.890(5) | 0.842(22) |
| C60d | 0.393(11) | 0.879(3) | 0.884(14) |
| W60 | 0.339(10) | 0.896(3) | 0.815(14) |
| C62a | 0.343(50) | 0.895(15) | 0.821(68) |
| W62a | 0.360(21) | 0.889(7) | 0.843(28) |
| W62b | 0.380(28) | 0.883(9) | 0.869(35) |
| W64 | 0.386(16) | 0.881(5) | 0.876(19) |
| C64 | 0.401(17) | 0.877(5) | 0.894(20) |

Table 5
Experimental and lattice values for J , L and R_{m_s} .

The ratio of the quark masses obtained with different methods is only function of J and L and experimental ratios. In particular the ratio of the strange quark mass obtained with (1) and (3) is

$$R_{m_s} = \frac{(m_s)_K}{(m_s)_\phi} = \frac{1}{C_{sl}^2(1 + \frac{1}{R})} \frac{2J}{\frac{M_s^{Exp}}{M_{K^*}} - L}. \quad (44)$$

where R is defined in eq. (32). In Table 5 we report the experimental value for $R_{m_s}^{Exp}$ and the values we have obtained for our lattices. R_{m_s} is a ratio of different definitions of lattice quark masses that does not suffer from $O(a)$ effects induced by renormalization constants and is related to experimental quantities. We believe that the difference $R_{m_s}^{Exp} - R_{m_s}^{Lat}$ is a good estimate of the overall systematic error on the strange quark mass. This error should essentially take into account both the quenching approximation and the $O(a)$ effects that we cannot a priori estimate.

4.3 Extraction of raw results for the charm quark mass

In order to obtain the charm quark mass we have to extrapolate the meson masses and the matrix elements both in the heavy and light quark masses. It is clear that in this case $O(ma)$ effects will be much more relevant than for the strange and light quarks. We use two different methods:

- (1) We first interpolate/extrapolate linearly the heavy-light pseudoscalar meson masses in the light quark mass to m_s extracted from (33). We then determine the charm quark mass by fixing the D_s -meson mass to its physical value and using the equation (4). The lattice charm quark masses obtained in this way for all lattices are reported in table 6. For the Axial Ward Identity ρ_c is given by

$$\rho_c = \rho|_{M_{PS}=M_{D_s}} - \rho_s \quad (45)$$

with ρ_s defined in eq. (35). The values obtained for all lattices are reported in table 7.

- (2) As in (1) but we determine the value of the charm quark mass by fixing the D_s^* -meson mass to its physical value.

As for the light quark masses, the two methods described above should give consistent results for m_c and ρ_c , apart from discretization errors and quenching effects. We shall use the spread between the two determinations as an estimate of the overall systematic error.

5 Physical Results for quark masses

On the basis of the discussion of previous sections, we now present the final results. From the lattice data of the left columns of tables 6 and 7, we obtain the PT and NP \overline{MS} results reported in the same tables.

In the PT case there is a large ambiguity in the choice among the lattice strong coupling constants which have been proposed to have a better convergence of the series. In the appendix we give in detail which definitions we have used. The difference among them is of course $O(\alpha_s^2)$ but on the lattice the behaviour of the perturbative series can be very bad [20]. The different values are averaged and the spread taken as an estimate of the error.

In the continuum we have used both in the PT and NP case eq. (47) with $n_f = 0$ and $\Lambda_{QCD} = 251 \pm 21 \text{ MeV}$ [29] as discussed in the appendix. We have checked that the final results change by less than 3% if we had used $n_f = 4$ and $\Lambda_{QCD} = 340 \pm 120 \text{ MeV}$, and this is only part of the error due to the quenching approximation which we cannot estimate.

The NP results contain only the statistical error on the matrix elements and renormalization constants. The AWI results are shown in figs. 1-4.

In the spectroscopy case we find a reasonable agreement between the NP and PT results that turn out to be compatible with previous determinations [6,7,10]. This is not the case for the AWI where the PT results are lower than the NP ones by more than two standard deviations. In our opinion this confirms that the perturbation theory fails in the determination of the pseudoscalar RC. On the other hand the NP results for different actions and methods are in very good agreement among them.

As far as the a dependence is concerned, for $\beta = 6.0$ and 6.2 the data are definitely stable, within the errors, for all methods. At $\beta = 6.4$ the data apparently show a slight decrease. Due to the small physical volume at this β value and the fact that this effect is present both in the Wilson and the Clover case we believe that one cannot disentangle volume and $O(a)$ effects in this lattice [7] and we will not take into account in any further result. With our present data an extrapolation in a is then out of reach.

The charm quark results appear to be quite more noisy than the light and strange ones. This supports the fact that at large masses order am contaminations are important.

To obtain final results, we average the non perturbative AWI results at $\beta = 6.0$ and 6.2 as independent ones. For the strange and charm quark, we also take into account the overall systematic error which we evaluate from the spread in

the quark masses extracted from different mesons as described in sec. 4. This error is also propagated to the light quark using eq. (34) and is the second one in eq. (46).

From NP renormalized AWI we obtain our final results

$$\begin{aligned}
\overline{m}^{\overline{MS}}(2\text{ GeV}) &= 5.7 \pm 0.1 \pm 0.8 \text{ Mev} \\
m_s^{\overline{MS}}(2\text{ GeV}) &= 130 \pm 2 \pm 18 \text{ Mev} \\
m_c^{\overline{MS}}(2\text{ GeV}) &= 1662 \pm 30 \pm 230 \text{ Mev} .
\end{aligned}
\tag{46}$$

which are reported in the abstract.

| Run | $\overline{m}a^{-1}$ | | $\overline{m}^{\overline{MS}}$ | | $m_s a^{-1}$ | | $m_s^{\overline{MS}}$ | | $m_c a^{-1}$ | | $m_c^{\overline{MS}}$ | |
|------|----------------------|--------|--------------------------------|-------|--------------|--------|-----------------------|-------|--------------|----------|-----------------------|-------|
| | NP | Pert. | NP | Pert. | NP | Pert. | NP | Pert. | NP | Pert. | NP | Pert. |
| C60a | 3.45(12) | - | 4.9(4) | | 78.9(22) | - | 113(8) | | - | - | - | - |
| C60b | 3.36(9) | - | 4.8(3) | | 77.3(17) | - | 110(7) | | - | - | - | - |
| C60c | 3.49(14) | - | 5.0(4) | | 79.4(25) | - | 113(8) | | - | - | - | - |
| C60d | 3.21(13) | - | 4.6(3) | | 74.7(26) | - | 107(7) | | - | - | - | - |
| W60 | 4.36(12) | 5.8(2) | 6.1(8) | | 97.9(20) | 129(4) | 137(17) | | 1335(31) | 1764(62) | 1865(247) | |
| C62a | 3.60(29) | - | 5.2(6) | | 81.1(41) | - | 117(9) | | 881(18) | - | 1275(90) | |
| W62a | 4.10(18) | 5.6(3) | 5.9(8) | | 93.3(29) | 127(5) | 134(17) | | 1205(24) | 1646(44) | 1730(212) | |
| W62b | 3.98(23) | 5.5(4) | 5.7(8) | | 91.8(39) | 126(6) | 132(17) | | 1206(32) | 1651(64) | 1738(222) | |
| W64 | 3.55(18) | 5.1(3) | 5.3(7) | | 82.0(35) | 119(6) | 123(17) | | - | - | - | |
| C64 | 2.86(17) | - | 4.3(4) | | 66.9(34) | - | 100(9) | | - | - | - | |

Table 6

Lattice quark masses and the corresponding \overline{MS} values in MeV at NLO from the pseudoscalar meson spectroscopy and a^{-1} from M_{K^*} . \overline{MS} masses are at a scale $\mu = 2$ GeV.

6 Conclusions

We have discussed the quark mass renormalization. We have calculated the quark masses from the meson spectroscopy and from the Axial Ward Identity using different sets of quenched data with $\beta = 6.0, 6.2$ and 6.4 and using the Wilson and the “improved” SW-Clover action. The data at $\beta = 6.4$ have been used only for an exploratory study as the physical volume and the time

| Run | $\bar{\rho}a^{-1}$ | | | $\bar{m}^{\overline{MS}}$ | | | $\rho_s a^{-1}$ | | | $m_s^{\overline{MS}}$ | | | $\rho_c a^{-1}$ | | | $m_c^{\overline{MS}}$ | | |
|------|--------------------|--------|--------|---------------------------|--------|---------|-----------------|----------|-----------|-----------------------|-------|---|-----------------|-------|---|-----------------------|-------|---|
| | NP | Pert. | | NP | Pert. | | NP | Pert. | | NP | Pert. | | NP | Pert. | | NP | Pert. | |
| C60a | 2.64(11) | 6.0(3) | 4.0(3) | 60.4(20) | 136(6) | 93(8) | - | - | - | - | - | - | - | - | - | - | - | - |
| C60b | 2.52(7) | 5.7(2) | 3.9(3) | 58.0(14) | 131(5) | 89(6) | - | - | - | - | - | - | - | - | - | - | - | - |
| C60c | 2.68(11) | 6.0(3) | 4.1(3) | 60.9(20) | 136(6) | 93(7) | - | - | - | - | - | - | - | - | - | - | - | - |
| C60d | 2.41(12) | 5.5(3) | 3.7(3) | 56.1(24) | 128(6) | 86(7) | - | - | - | - | - | - | - | - | - | - | - | - |
| W60 | 3.48(11) | 5.7(2) | 4.3(5) | 78.2(20) | 127(5) | 98(11) | 1091(30) | 1777(67) | 1362(160) | - | - | - | - | - | - | - | - | - |
| C62a | 2.83(23) | 6.0(5) | 4.4(5) | 63.6(33) | 134(8) | 99(9) | 820(36) | 1725(93) | 1269(113) | - | - | - | - | - | - | - | - | - |
| W62a | 3.47(14) | 5.6(3) | 4.5(5) | 78.9(23) | 126(5) | 102(11) | 1012(21) | 1624(43) | 1311(144) | - | - | - | - | - | - | - | - | - |
| W62b | 3.32(19) | 5.3(3) | 4.3(5) | 76.5(32) | 124(6) | 99(12) | 1001(29) | 1610(66) | 1301(149) | - | - | - | - | - | - | - | - | - |
| W64 | 3.19(17) | 4.9(3) | 4.3(5) | 73.7(33) | 114(6) | 100(13) | - | - | - | - | - | - | - | - | - | - | - | - |
| C64 | 2.41(14) | 4.7(3) | 3.8(4) | 56.3(27) | 110(6) | 90(8) | - | - | - | - | - | - | - | - | - | - | - | - |

Table 7

Lattice quark masses and the corresponding \overline{MS} values at NLO, in MeV from the Axial Ward Identity and a^{-1} from M_{K^*} . \overline{MS} masses are at a scale $\mu = 2$ GeV.

extension of the lattice may be too small to be reliable.

Perturbation theory appears to fail giving inconsistent results for the two methods. The results for independent NP methods are well consistent and stable strongly supporting the reliability of our final results reported in the abstract. In the β range that we have considered and with our statistics, we do not believe that one can safely extrapolate to the continuum limit both for the Wilson and the SW-Clover action.

7 Appendix

In this appendix we shall describe the different definition of the lattice strong coupling constant that we have used for the PT results.

The running coupling constant in \overline{MS} scheme is:

$$\frac{\alpha_s(\mu^2)}{4\pi} = \frac{1}{\beta_0 \ln(\mu^2/\Lambda_{QCD}^2)} \left\{ 1 - \frac{\beta_1 \ln[\ln(\mu^2/\Lambda_{QCD}^2)]}{\beta_0^2 \ln(\mu^2/\Lambda_{QCD}^2)} \right\} + \dots, \quad (47)$$

this is related to the bare lattice coupling $\alpha_s^L(a) = g_L^2(a)/4\pi$ by the relation:

$$\frac{1}{\alpha_s^L(a)} = \frac{1}{\alpha_s(q)} \left\{ 1 + \frac{\alpha_s(q)}{4\pi} \left[\beta_0 \ln\left(\frac{\pi}{qa}\right)^2 + 48.76 \right] \right\}. \quad (48)$$

In ref. [20] a new expansion parameter, $\alpha_s^{V_1}$ has been introduced based on the heavy quark potential:

$$\frac{1}{\alpha_s^L(a)} = \frac{1}{\alpha_s^{V_1}(q)} \left\{ 1 + \frac{\alpha_s^{V_1}(q)}{4\pi} \left[\beta_0 \ln\left(\frac{\pi}{qa}\right)^2 + 59.09 \right] \right\}, \quad (49)$$

using the perturbative expansion for the trace of the plaquette one obtains, [20]:

$$\frac{1}{\alpha_s^L(a)} = \frac{1}{\alpha_s^{V_1}(\pi/a) \langle \frac{1}{3} \text{Tr} U_P \rangle} \left[1 + \frac{\alpha_s^{V_1}(\pi/a)}{4\pi} 6.45 \right]. \quad (50)$$

where U_P is the plaquette. The third definition that we have used is:

$$\frac{1}{\alpha_s^L(a)} = \frac{(8k_c)^4}{\alpha_s^{V_2}} \quad (51)$$

where k_c is the critical value of the hopping parameter.

In our analysis we have used α_s , $\alpha_s^{V_1}$, $\alpha_s^{V_2}$ as they have been used in the literature in the past. One should note that each definition has different $O(a)$ effects and eq. (51) is only valid at the LO while eqs. (47-50) are valid up to NLO. We have made this choice as it is the same done in ref. [6] and so the results can immediately be compared.

We have evaluated all cases both in the quenched and unquenched case. In the latter case the value of $\Lambda_{QCD}^{n_f}$ at the various scales is obtained from the SLD-LEP result $\Lambda_{QCD}^5 = 240 \pm 90 \text{ MeV}$ [27] by matching the strong coupling constant at n_f and $n_f + 1$ at the threshold of the new flavour [30]. In the quenched case we have used $\Lambda_{QCD} = 251 \pm 21 \text{ MeV}$ [29]. Furthermore we have also chosen two different scales used to evaluate the strong coupling constant, i.e. $\alpha_s(\pi/a)$ and $\alpha_s(1/a)$. All these results have been averaged and the spread taken as the error. We have also done this analysis using $\Lambda_{QCD} = 340 \pm 120 \text{ MeV}$ and we find that the final average changes by less than 5% which is well within the error. As an example α_s^{MS} changes from 0.20 to 0.31 at a scale $\mu = 1/a = 2 \text{ GeV}$ which leads to a change in the correction of that order.

Acknowledgements

We wish to thank the APE collaboration for allowing us to use the lattice correlation functions presented here. We warmly thank C. R. Allton, V. Lubicz, E. Franco, G. Martinelli, M. Testa and A. Vladikas for enlightening discussions. We also acknowledge the use of C. R. Allton's analysis program. M.T. acknowledges the support of PPARC through grant GR/L22744.c

References

- [1] H. Leutwyler, Nucl. Phys. B 337, (1990) 108 and references therein.
H. Leutwyler, Phys. Lett. B 378, (1996) 313.
- [2] J. Bijnens, J. Prades and E. de Rafael, Phys. Lett. B 348 (1995) 226.
- [3] M. Jamin and M. Münz, Z. Phys. C 66 (1995) 633.
- [4] P. Colangelo, F. De Fazio, G. Nardulli, N. Paver, Phys. Lett. B 408 (1997) 340.
- [5] C.A. Dominguez, Proceedings of the 16th International Workshop on Weak Interactions and Neutrinos (WIN 97), Capri, Italy, 1997.
- [6] C. R. Allton et al., Nucl. Phys. B 431 (1994) 667.
- [7] C.R. Allton, V. Giménez, L. Giusti and F. Rapuano,
Nucl. Phys. B 489, (1997) 427.
- [8] JLQCD Collaboration (S. Aoki et al.), Nucl. Phys. B (Proc. Suppl.) 63 (1998) 275.
- [9] CP-PACS Collaboration (S. Aoki et al.),
Nucl. Phys. B (Proc. Suppl.) 63 (1998) 161,
Nucl. Phys. A (Proc. Suppl.) 60 (1998) 14.
- [10] T. Bhattacharya and R. Gupta, Phys. Rev D 55 (1997) 7203,
Nucl. Phys. B (Proc. Suppl.) 63 (1998) 95.
- [11] B. J. Gough et al., Phys. Rev. Lett. 79 (1997) 1622.
- [12] SESAM-Collaboration (N. Eicker et al.), Phys. Lett. B 407 (1997) 290.
- [13] B. Sheikholeslami, R. Wohlert, Nucl. Phys. B259 (1985) 572.
- [14] G. Heatlie et al., Nucl. Phys. B352 (1991) 266, Nucl. Phys. B (Proc. Suppl.) 17 (1990) 607.
- [15] L.H. Karsten and J. Smit, Nucl. Phys. B 183 (1981) 103.
M. Bochicchio et al., Nucl. Phys. B 262 (1985) 331.

- [16] E. Gabrielli et al, Nucl. Phys. B 362 (1991) 475.
A. Borrelli, C. Pittori, R. Frezzotti and E. Gabrielli, Nucl. Phys. B 409 (1993) 382.
- [17] M. Crisafulli, V. Lubicz and A. Vladikas, Eur. Phys. J. C 4 (1998) 145.
- [18] M. Lüscher, S. Sint, R. Sommer and P. Weisz, Nucl. Phys. B 478 (1996) 365.
- [19] G. Martinelli and Y.C. Zhang, Phys. Lett. B 123 (1983) 433.
H. W. Hamber and C. M. Wu, Phys. Lett. B 133 (1983) 351.
- [20] G.P. Lepage and P.B. Makenzie, Phys. Rev D 48 (1993) 2250.
- [21] G.Martinelli *et al.*, Nucl. Phys. B 445 (1995) 81.
- [22] K. Jansen et al., Phys. Lett. B372 (1996) 275.
M. Lüscher et al., hep-ph/9711205.
- [23] V. Giménez, L. Giusti, F. Rapuano, M. Talevi, hep-lat/9806006, to be published in Nucl. Phys. B.
- [24] C. Parrinello, S. Petrarca and A. Vladikas, Phys. Lett. B 268 (1991) 236.
L. Giusti, Nucl. Phys. B 498 (1997) 331.
- [25] T χ L Collaboration (N. Eicker et al.), Nucl. Phys. B (Proc. Suppl.) 60A (1998) 311 and work in progress.
- [26] C. R. Allton et al., Phys. Lett. B405 (1997) 133.
- [27] Particle Data Group, Phys. Rev D 54 (1996) 1.
- [28] UKQCD Collaboration (P. Lacock et al.), Phys. Rev D 52 (1995) 5213.
- [29] S. Capitani et al., Nucl. Phys. B (Proc. Suppl.) 63 (1998) 153.
- [30] W. Marciano, Phys. Rev D 29 (1984) 580.

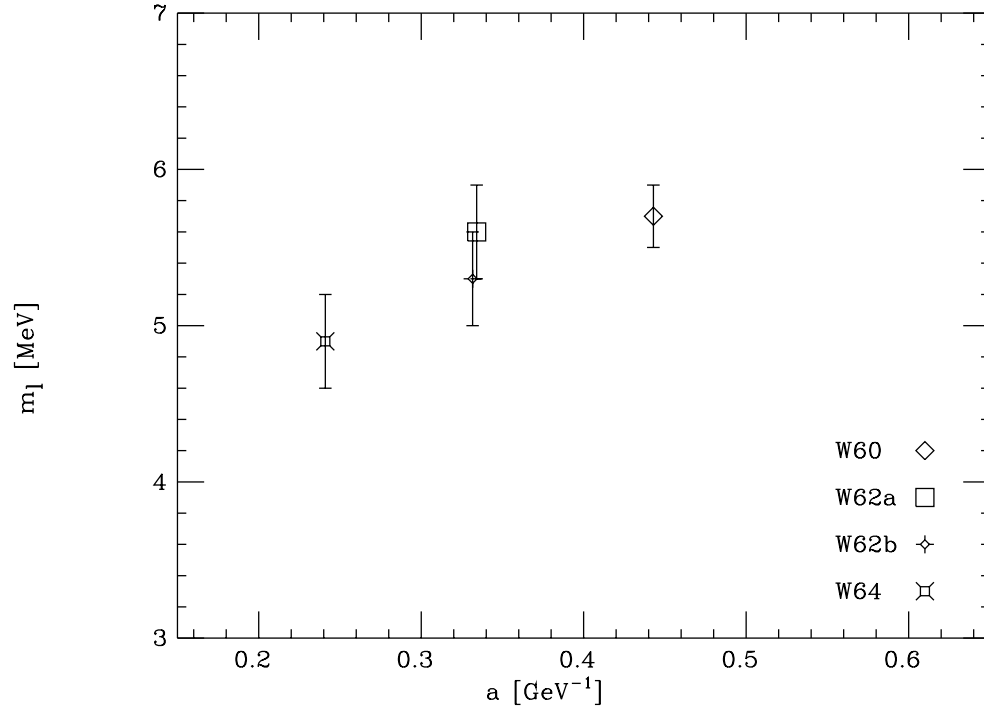


Fig. 1. Non-perturbatively renormalized quark masses $\overline{m}^{\overline{MS}}$ for all Wilson lattices from the Axial Ward Identity

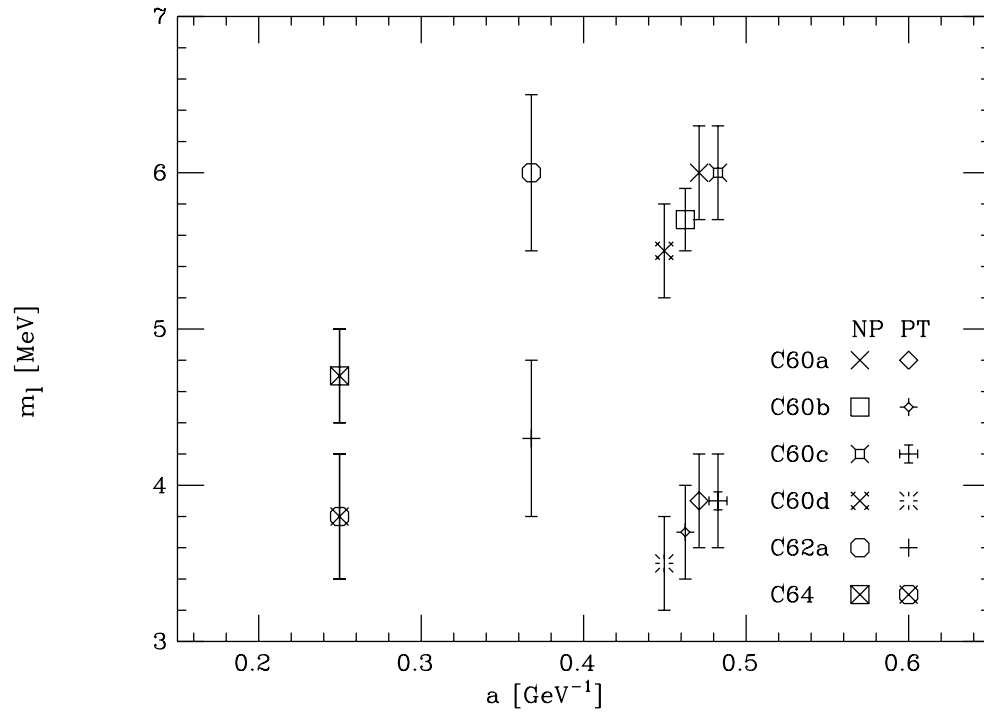


Fig. 2. Non-perturbatively renormalized quark masses $\overline{m}^{\overline{MS}}$ for all SW-Clover lattices from the Axial Ward Identity

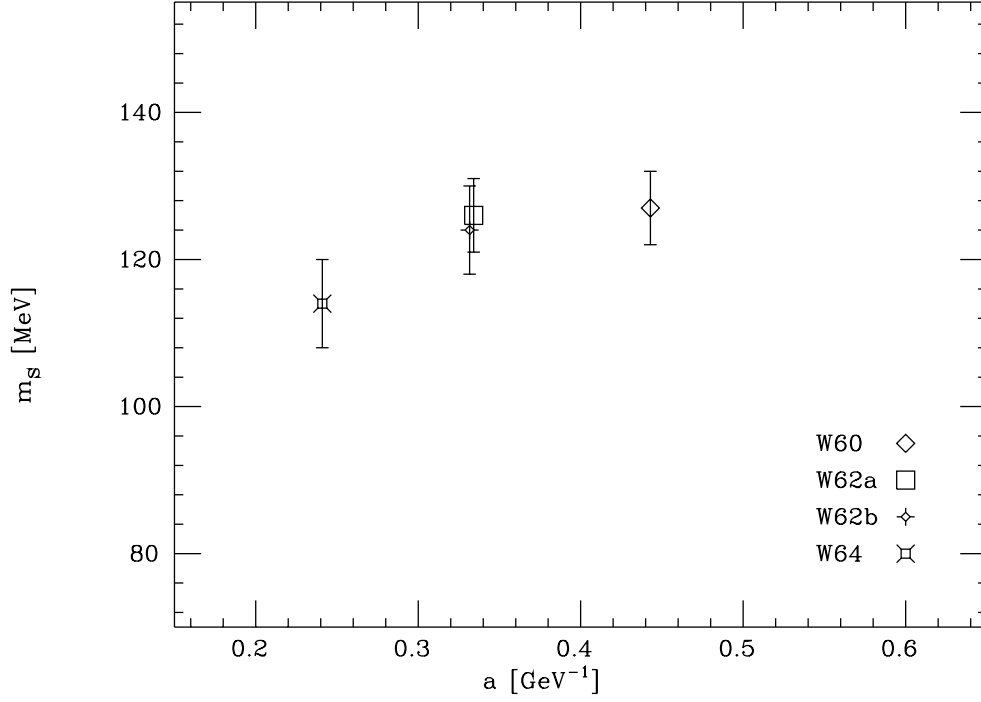


Fig. 3. Non-perturbatively renormalized quark masses $m_s^{\overline{MS}}$ for all Wilson lattices from the Axial Ward Identity

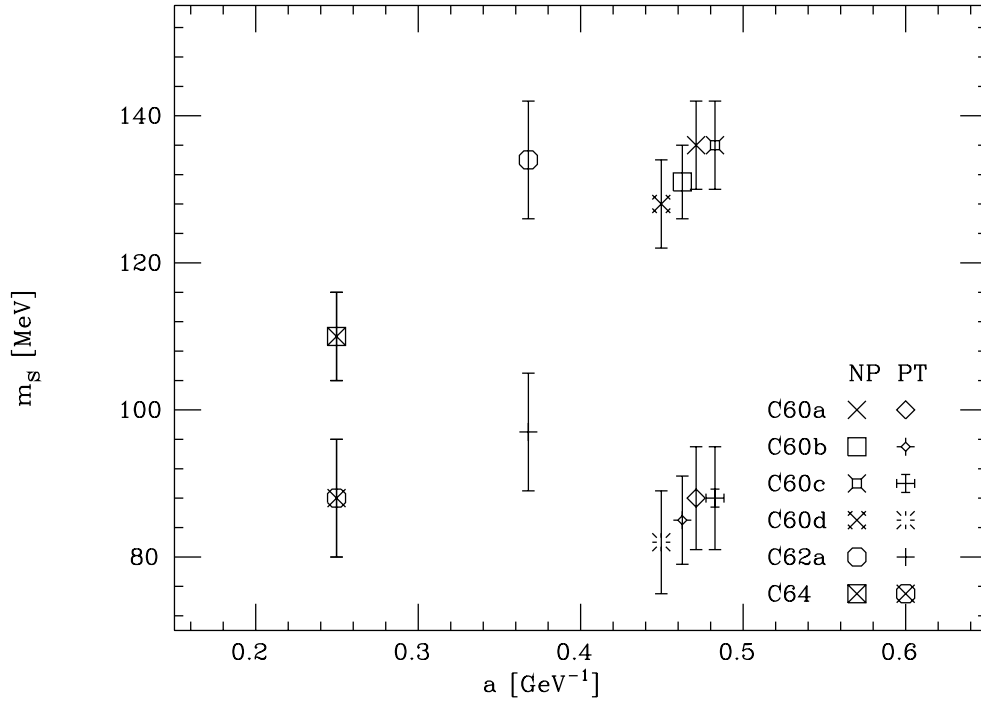


Fig. 4. Non-perturbatively renormalized quark masses $m_s^{\overline{MS}}$ for all SW-Clover lattices from the Axial Ward Identity